Identification of 12/15-lipoxygenase as a suppressor of myeloproliferative disease

Melissa Kristine Middleton,[1,2] Alicia Marie Zukas,[1] Tanya Rubinstein,[1] Michele Jacob,[1] Peijuan Zhu,[3,4] Liang Zhao,[1] Ian Blair,[3,4] and Ellen Puré[1,2,5]

[1]The Wistar Institute, Philadelphia, PA 19104
[2]Immunology Graduate Group, [3]Center for Cancer Pharmacology, and [4]Institute for Translational Medicine and Therapeutics, University of Pennsylvania, Philadelphia, PA 19104
[5]The Ludwig Institute for Cancer Research, Philadelphia, PA 19104

Though Abl inhibitors are often successful therapies for the initial stages of chronic myelogenous leukemia (CML), refractory cases highlight the need for novel molecular insights. We demonstrate that mice deficient in the enzyme 12/15-lipoxygenase (12/15-LO) develop a myeloproliferative disorder (MPD) that progresses to transplantable leukemia. Although not associated with dysregulation of Abl, cells isolated from chronic stage 12/15-LO–deficient (Alox15) mice exhibit increased activation of the phosphatidylinositol 3–kinase (PI3-K) pathway, as indicated by enhanced phosphorylation of Akt. Furthermore, the transcription factor interferon consensus sequence binding protein (ICSBP) is hyperphosphorylated and displays decreased nuclear accumulation, translating into increased levels of expression of the oncoprotein Bcl-2. The ICSBP defect, exaggerated levels of Bcl-2, and prolonged leukemic cell survival associated with chronic stage Alox15 MPD are all reversible upon treatment with a PI3-K inhibitor. Remarkably, the evolution of Alox15 MPD to leukemia is associated with additional regulation of ICSBP on an RNA level, highlighting the potential usefulness of the Alox15 model for understanding the transition of CML to crisis. Finally, 12/15-LO expression suppresses the growth of a human CML–derived cell line. These data identify 12/15-LO as an important suppressor of MPD via its role as a critical upstream effector in the regulation of PI3-K–dependent ICSBP phosphorylation.

CORRESPONDENCE
Ellen Puré:
pure@wistar.org

Abbreviations used: 12/15-LO, 12/15-lipoxygenase; CML, chronic myelogenous leukemia; H&E, hematoxylin and eosin; HETE, hydroxyeicosatetraenoic acid; HODE, hydroxyoctadecadienoic acid; HpETE, hydroperoxyeicosatetraenoic acid; ICSBP, interferon consensus sequence binding protein; IRF-8, interferon regulatory factor 8; MPD, myeloproliferative disease; PI3-K, phosphatidylinositol 3–kinase.

Leukemia results from genetic defects that lead to enhanced proliferation and survival of bone marrow–derived cells, disrupting homeostasis in the hematopoietic compartment. Chronic myelogenous leukemia (CML) is a malignant myeloproliferative disease (MPD) that comprises 15–20% of hematopoietic cancers in humans (1). It is typified by an initial chronic stage, during which patients experience splenomegaly secondary to myeloid cell expansion. This relatively benign phase of the disease often progresses to a fatal blast crisis within 3–5 yr of diagnosis (1). The Philadelphia chromosome, the consequence of a t(9;22) (q34;q11) translocation, is a hallmark of the majority of human CML (2) and results in a fusion between *bcr* and the tyrosine kinase *abl*. The product of the *Bcr-Abl* fusion is altered in its cellular distribution and exhibits constitutive tyrosine kinase activity compared with c-Abl. Consequently, hyperphosphorylation of key Bcr-Abl substrates promotes leukemogenesis in myeloid cells (2).

Exciting advances in molecular medicine have yielded imatinib mesylate/STI571/Gleevec, an inhibitor of Abl activity, which has proved to be effective in many patients with CML (3). Unfortunately, a subset of patients afflicted with myeloid leukemias initially exhibit imatinib resistance, whereas others become refractory to treatment owing to development of drug resistance caused by subsequent mutations in *abl* (4–7). Moreover, evolution of CML to blast crisis is characterized by the development of a degree of resistance to treatment that is notoriously difficult to overcome (1, 6, 8). The survival of STI571-resistant leukemic cells can be mediated by compensatory activation of the Ras/mitogen-activated protein kinase and phosphatidylinositol 3–kinase (PI3-K)/Akt signaling cascades (9, 10). Thus, targeting these pathways may not only treat leukemic disease but can also circumvent the development of STI571 resistance.

The online version of this article contains supplemental material.

Though several elegant mouse models have been developed to study myeloid leukemias (11–14), many of these develop fulminant blast crisis within weeks of induction, limiting their usefulness for investigating the chronic phase of CML and the critical transition to blast crisis phase (2). One of the few exceptions is the MPD observed in mice deficient in interferon consensus sequence binding protein/interferon regulatory factor 8 (ICSBP/IRF-8), which is characterized by more gradual and less frequent transitions to leukemic blast crisis (15). Importantly, the loss of ICSBP expression in patients with CML correlates with disease progression (16), whereas forced expression induces apoptosis in cell lines established from patients with Bcr-Abl$^+$ CML (17, 18), even in cells which are STI571 resistant (19). However, despite the importance of ICSBP in human CML, none of the regulatory pathways upstream of ICSBP have been defined in the context of leukemia. In this study, we demonstrate that 12/15-lipoxygenase (12/15-LO) regulates ICSBP, and thereby MPD, in a PI3-K–dependent manner.

Lipoxygenases are enzymes that incorporate oxygen into unsaturated lipids and are named according to the position of the carbon double bonds they oxidize (20). These reactions yield short-lived peroxidized products, such as 12*(S)*-hydroperoxyeicosatetraenoic acid (12*(S)*-HpETE) and 13*(S)*-hydroperoxyoctadecadienoic acid, which reduce or are actively converted to several different products, including 12*(S)*-hydroxyeicosatetraenoic acid (12*(S)*-HETE), 13*(S)*-hydroxyoctadecadienoic acid (13*(S)*-HODE), lipoxins, and hepoxilins. Importantly, the levels of the lipoxygenase product derivative 12*(S)*-HETE are reduced in patients with CML compared with normal controls (21), suggesting a role for lipoxygenase activity in the suppression of this disease. Consistent with this hypothesis, expression of platelet 12-lipoxygenase (encoded by Alox12) inversely correlates

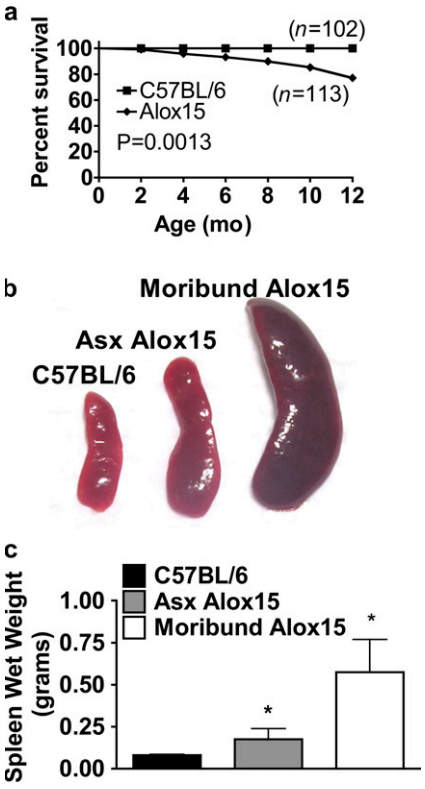

Figure 1. Decreased survival and marked splenomegaly in 12/15-LO–deficient mice. (a) Kaplan-Meier plot of 102 wild-type (B6) and 113 Alox15 mice representing a nearly 1:1 ratio of males/females. (b) Representative spleens of 10–12-wk-old wild-type, asymptomatic (Asx), and moribund Alox15 mice. (c) Mean wet weights ± SD of the spleens shown in b ($n = 18$ for B6 and Asx Alox15 mice; $n = 9$ for moribund Alox15 mice). *, $P < 0.0001$.

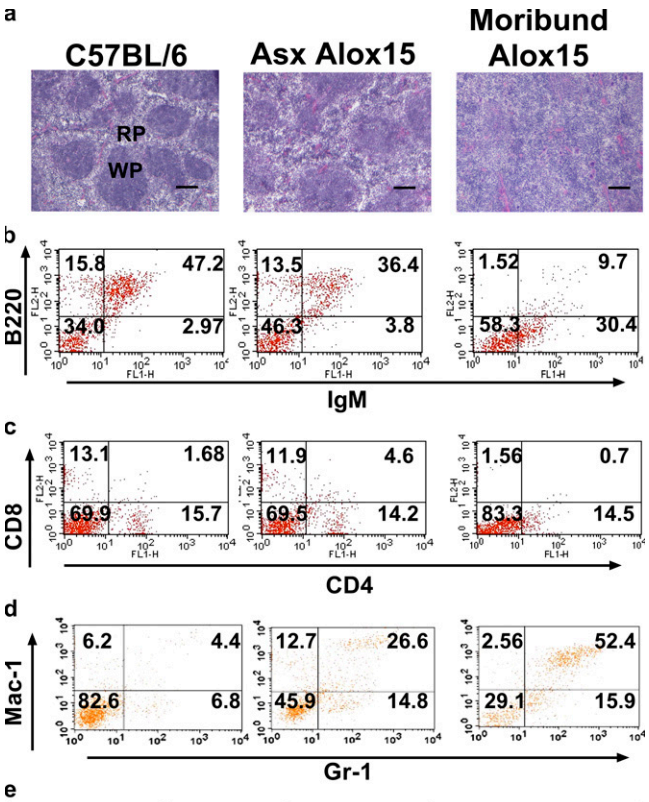

e

Cell type	C57BL/6	Asx Alox15	Moribund Alox15
Lymphocytes	90-155	48-52	18-30
Monocytes	2-9	1-2	0-3
Granulocytes	4-7	50-60	80-114

Figure 2. Disrupted architecture and increased myeloid cells in the spleens of 12/15-LO–deficient mice. (a) H&E staining of 8-μm frozen sections of spleens from wild-type ($n \geq 10$), Asx Alox15 ($n \geq 10$), and moribund Alox15 mice ($n = 7$). WP, white pulp; RP, red pulp. Bar, 50 μm. Fluorescence-activated flow cytometric analysis of (b) B cell populations, (c) T cell populations, and (d) myeloid populations in isolated splenocytes of representative samples gated on live cells. Percentages for each quadrant are indicated. Mac-1/GR-1 double-positive cells increased from a range of 1.8–8.2% in wild-type ($n = 11$) to 15–24% and 35–70% in the spleens of Alox15 mice in the chronic ($n = 9$) and crisis ($n = 4$) phases, respectively. (e) Differential counts of cytospin preparations of splenocytes from asymptomatic (Asx) and moribund Alox15 mice versus wild-type controls.

with the severity of CML disease (22). Similarly, leukocyte 12/15-LO (encoded by Alox15) is located on a region of human chromosome 17 implicated in the suppression of myeloid leukemogenesis (23). Despite these intriguing data, no direct evidence had yet supported a role for lipoxygenases in regulating leukemogenesis. While conducting experiments with 12/15-LO–deficient (Alox15) mice, we discovered that they develop an indolent MPD akin to human CML. We now provide the first description of Alox15 mice as a model for MPD and demonstrate that the pathology in these animals is related to 12/15-LO–mediated PI3-K–dependent regulation of ICSBP and its downstream target genes in vivo.

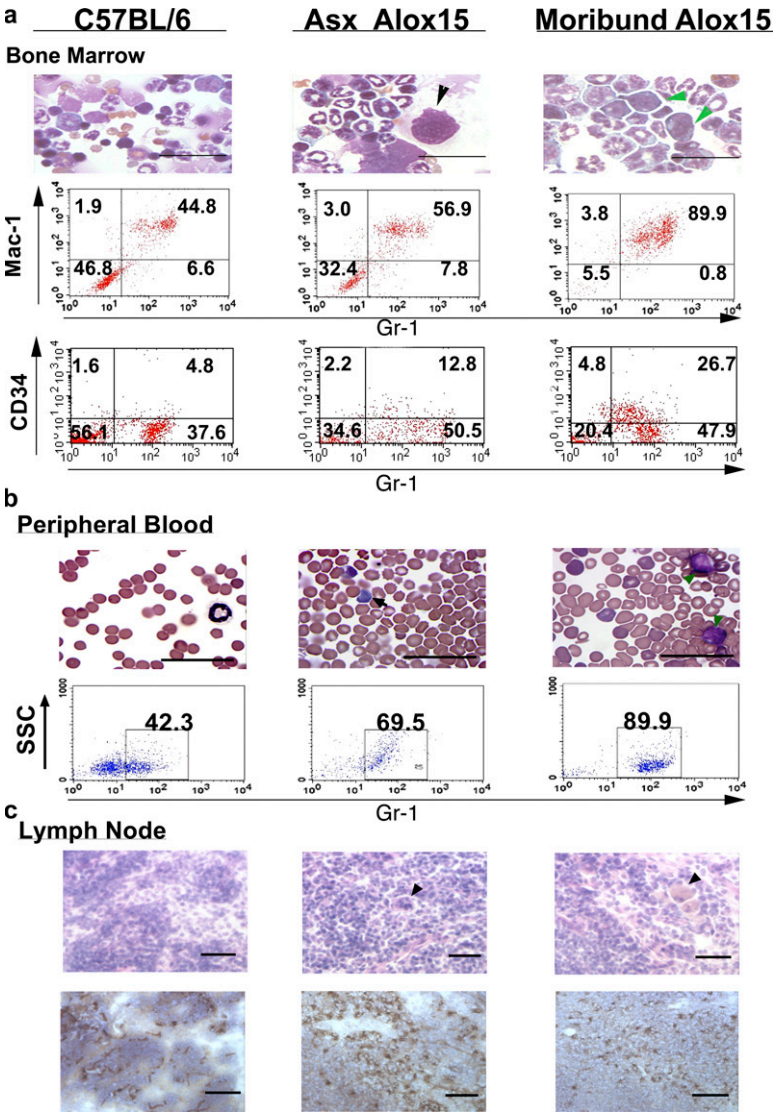

Figure 3. Increased myeloid cells in the bone marrow, blood, and lymph node of 12/15-LO–deficient mice. (a, top) Representative ($n = 6$) wild-type (B6) and Alox15 bone marrow cells. Note the large megakaryocyte (black arrowhead) in the asymptomatic (Asx) Alox15 cells. Green arrowheads indicate myeloblasts. Note the presence of basophilic cytoplasm, prominent nucleoli, undefined granules, and the absence of Auer rods (Auer rods would support a diagnosis of acute myeloid leukemia; reference 56). Bar, 50 μm. (a, middle) Representative flow cytometric analysis of Mac-1 and Gr-1 expression in bone marrow. Percentages for each quadrant are indicated. Double-positive ranges: C57BL/6, 35.9–52.7% ($n = 7$); Asx Alox15, 43.8–61.2% ($n = 7$); and moribund Alox15, 61.9–90.1% ($n = 5$). (a, bottom) Gr-1 and CD34 expression in bone marrow. Percentages for each quadrant are indicated. Double-positive ranges: C57BL/6, 4.5–9.1% ($n = 5$); Asx Alox15, 11.2–17.9 ($n = 4$); and moribund Alox15, 25.8–33.1% ($n = 3$). (b, top) C57BL/6 and Alox15 blood smears. Note the platelet anisocytosis and micromegakaryocytosis often found in CML. Black arrows point to examples of basophils, and green arrowheads indicate example blast cells. Bar, 50 μm. (b, bottom) Flow cytometric analysis of Gr-1 expression in blood leukocytes from 25-wk-old B6, Asx Alox15, and moribund Alox15 mice. Percentages of Gr-1$^+$ cells are indicated. Gr-1$^+$ ranges: B6, 42.5–51% ($n = 5$); Asx Alox15, 62–79.2% ($n = 5$); and moribund Alox15, 68.2–90.% ($n = 3$). (c, top) H&E-stained sections of wild-type and chronic Alox15 lymph node. Arrowheads point to pseudo-Gaucher–like cells. (c, bottom) Immunohistochemical staining for Gr-1$^+$ cells in B6 and Alox15 lymph node. Bar, 50 μm.

RESULTS

12/15-LO–deficient mice develop a MPD

Though we observed no gross differences in the tissue composition of Alox15 mice compared with wild-type controls at 6–8 wk of age (Fig. S1, available at http://www.jem.org/cgi/content/full/jem.20061444/DC1), we noted a small but distinct increase in the death rate of homozygous knockout animals as they aged compared with wild-type controls (Fig. 1 a). Furthermore, examination of outwardly healthy Alox15 mice older than 8 wk revealed varying degrees of splenomegaly with 100% penetrance compared with wild-type controls (Fig. 1, b and c). Early morbidity and mortality was associated with increasingly severe splenomegaly (Fig. 1, b and c).

Analysis of splenic architecture revealed a remarkable decrease in the number of follicles and disrupted compartmentalization of the red and white pulp in the asymptomatic Alox15 compared with wild-type mice (Fig. 2 a). Strikingly, severe splenomegaly in moribund Alox15 mice was characterized by complete loss of splenic compartmentalization (Fig. 2 a). Phenotypic analysis of wild-type and Alox15 splenocytes by flow cytometry revealed a selective increase in the Mac-1^+/GR-1^+ (myeloid) population (Fig. 2, b–d), whereas differential counts of cytospin preparations of splenocytes from Alox15 mice versus wild-type controls demonstrated no expansion of other cell types (Fig. 2 e). Bone marrow was also affected, where the numbers of myeloid cells and their CD34$^+$/Gr-1^{lo} progenitors (24), as well as megakaryocytes (25), were increased at the expense of erythropoiesis (Fig. 3 a and Fig. S2, available at http://www.jem.org/cgi/content/full/jem.20061444/DC1). Moribund animals regularly demonstrated more than 25% myeloblast cells in the bone marrow by morphology and CD34 expression (thus, these animals are herein referred to as being in blast crisis stage).

Asymptomatic Alox15 mice, whose spleens were at least twice the weight of wild-type controls, as well as all of those in the crisis stage, also displayed blood leukocytosis and basophilia, with myeloblasts apparent in the moribund mice (Fig. 3 b). Furthermore, though the lymph nodes were not grossly enlarged, they exhibited progressive hypercellularity and morphological changes, with pseudo-Gaucher cells present (Fig. 3 c) (26). Immunohistochemistry revealed a marked increase in the proportion of GR-1^+ cells in lymph node in both asymptomatic and moribund compared with wild-type animals (Fig. 3 c). We also detected myeloid infiltrates in the skin of most moribund Alox15 mice that correlated with the development of dermatitis (Fig. S3, available at http://www.jem.org/cgi/content/full/jem.20061444/DC1), a poor prognostic sign in human CML (27). In contrast, other tissues (liver, kidney, lungs, and heart) displayed no evidence of pathology (unpublished data).

Overall, the data up to this point indicate that Alox15 mice develop a MPD. Considering the pathology described, including the percentage of myeloblasts in the bone marrow, we classified 10 wk and older asymptomatic Alox15 mice with less severe pathology as being in the chronic phase (~85% of the population) and the moribund mice (~15% of the population) as being in crisis phase. Furthermore, the pathology observed in these mice suggests that the most likely cause of death in the moribund mice was the severe anemia in these animals (Fig. S2).

12/15-LO activity suppresses proliferation and survival in mouse and human myeloid cells

We observed significantly increased proliferative capacity in splenic Alox15 myeloid cells based on cell cycle analysis (Fig. 4, a and b). In addition, the percentage of apoptotic cells was decreased in Alox15 compared with wild-type cells,

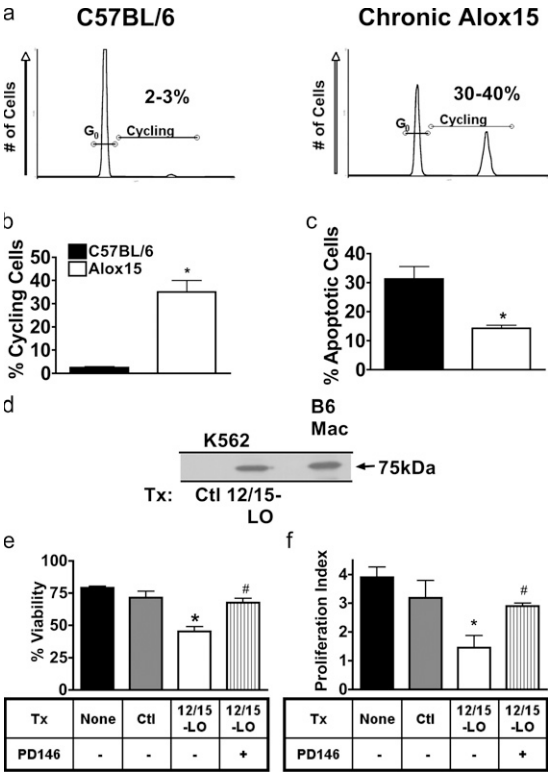

Figure 4. 12/15-LO suppresses proliferation and survival in mouse and human cells. (a) Flow cytometric analysis of propidium iodide–stained wild-type (B6) and chronic Alox15 (Chr) sorted Gr-1^+ splenocytes. (b) Quantification of data shown in panel a. *, P = 0.01 compared with B6 ($n = 3$). (c) The percentage of apoptotic cells in B6 and Alox15 myeloid cells from 10–20-wk-old B6 and Alox15 mice after 24-h culture was quantified using propidium iodide staining. *, P = 0.002 compared with B6 ($n = 4$). (d) Immunoblot of 12/15-LO in K562 cells transfected with a vector control or mouse 12/15-LO, as compared with sorted B6 splenic macrophages (Mac). An anti–human 12/15-LO antibody that cross reacts with mouse (not depicted) was used. Samples were normalized for protein concentration. (e) The number of viable K562 cells 24 h after transfection (Tx) with 12/15-LO or vector control (Ctl) in the presence of 10 μM PD146176 (PD146) or DMSO vehicle control was quantified using trypan blue exclusion. *, P = 0.0268 compared with Ctl DMSO ($n = 3$); #, P = 0.0256 compared with 12/15-LO DMSO ($n = 3$). (f) Proliferation index after 24 h of transfected K562 cells, as measured by the fold increase in viable cells treated with 10 μM PD146176 or DMSO vehicle control. *, P = 0.0149 compared with Ctl DMSO ($n = 3$); #, P = 0.005 compared with 12/15-LO DMSO vehicle. All error bars represent means ± SD.

indicating enhanced survival of Alox15 cells (Fig. 4 c). We then investigated the relevance of 12/15-LO to human MPD. Consistent with the potential role of 12/15-LO in suppressing human disease, we found that human Bcr-Abl$^+$ leukemia K562 cells (28), despite being derived from the myeloid lineage (which generally expresses 12/15-LO), do not express detectable levels of 12/15-LO protein (Fig. 4 d). However, forced expression resulted in levels of 12/15-LO similar to those found in mouse macrophages (Fig. 4 d) and led to a decrease in cell survival and proliferation that could be overcome by treatment with the 12/15-LO inhibitor PD146176 (Fig. 4, e and f). Thus, 12/15-LO can suppress human as well as mouse MPD.

The MPD in 12/15-LO–deficient mice is cell autonomous

To assess whether the MPD in Alox15 tissues fit the classification of a leukemia (29), we tested whether the Alox15 phenotype was cell autonomous by transplanting Alox15 cells into syngeneic, nonirradiated wild-type mice. The splenic enlargement and disrupted compartmentalization, as well as the myeloid cell expansion, we observed in Alox15 mice was uniformly recapitulated in wild-type recipients transplanted with crisis stage splenocytes or bone marrow cells as early as 4 wk after transfer (Fig. 5, a–c). Though transplant of cells from 10–12-wk-old chronic stage Alox15 mice did not result in overt pathology in wild-type recipients, the cells from these mice were transplantable to mice with severe combined immunodeficiency in 4 out of 6 cases (Fig. 5 c). Moreover, though it was not possible to assess clonality of the transferred cells, persistence of Alox15 cells in the donor mice was confirmed by PCR for the neomycin cassette introduced by the Alox15 targeting vector (Fig. 5 d). We conclude from these data that Alox15 mice develop a MPD that transitions to a transplantable leukemia in a subset of animals over time.

Role of 12/15-LO lipid mediators in suppressing leukemogenesis

To address the potential role of lipid mediators in 12/15-LO's impact on myeloid proliferation, we measured the lipid products released ex vivo during whole organ culture of Alox15 versus wild-type spleens. We found that Alox15 mice produced comparable amounts of 15*(S)*-HETE, lipoxin A_4, and 5*(S)*-HETE (a 5-lipoxygenase product) but reduced levels of 12*(S)*-HETE and 13*(S)*-HODE compared with wild-type controls (Fig. 6, a–e), indicating that 12*(S)*-HETE and 13*(S)*-HODE or their intermediates are the most likely lipid products to be involved in 12/15-LO–mediated suppression of leukemogenesis. This is consistent with the observation that a stable analogue of the 12*(S)*-HpETE derivative, hepoxilin A_4, can suppress the growth of K562 cells in in vivo models (30). Indeed, we found that 12*(S)*-HpETE displayed a modest ability to suppress viability in Alox15 and K562 cells (Fig. 6 f). The effects of 12*(S)*-HpETE on viability may, however, be minimized in these studies because of its lability and potential to act in synergy with other 12/15-LO products in vivo.

Alox15 MPD is Abl independent

Others have demonstrated that Abl hyperactivity in myeloid cells, associated with v-Abl or Bcr-Abl, can induce MPD in mice (12, 31). These studies compelled us to explore whether 12/15-LO expression may prevent MPD by suppressing endogenous Abl activity. To do this, we used concentrations of the Abl inhibitor STI571 sufficient to inhibit endogenous Abl activity. We found that, in contrast to the K562 cells (Fig. 7 a), Alox15 splenocytes did not undergo cell cycle arrest or apoptosis upon treatment with the Abl inhibitor STI571/imatinib (Fig. 7 b). We also used the endogenous Abl substrate Crk (32), rather than the pathologic Bcr-Abl

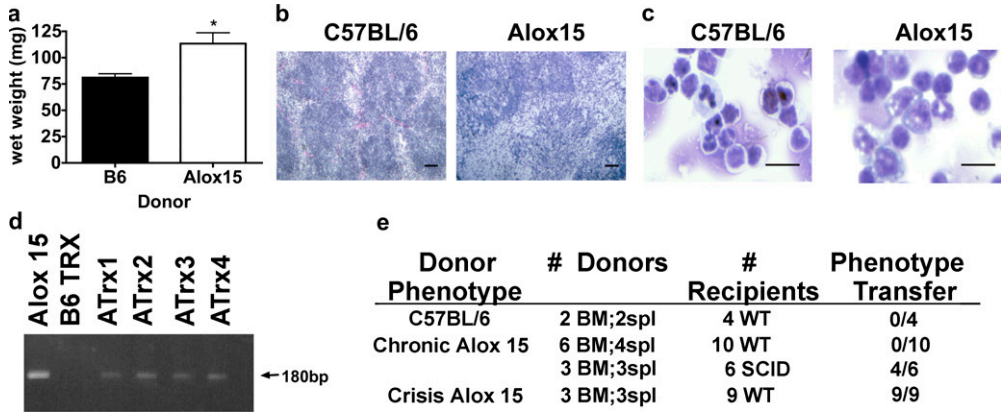

Donor Phenotype	# Donors	# Recipients	Phenotype Transfer
C57BL/6	2 BM;2spl	4 WT	0/4
Chronic Alox 15	6 BM;4spl	10 WT	0/10
	3 BM;3spl	6 SCID	4/6
Crisis Alox 15	3 BM;3spl	9 WT	9/9

Figure 5. The MPD in 12/15-LO–deficient mice is cell autonomous. (a) Increased splenic weight, (b) representative H&E-stained cryostat sections of spleens, and (c) cytospins of splenocytes from 8–10-wk-old wild-type mice injected via the tail vein with 0.5×10^6 (Alox15 crisis) or 10^7 (Alox15 chronic and C57BL/6) splenocytes or 2×10^6 bone marrow cells, monitored every other day, and killed at 6 or 10 wk after transfer. Bar, 50 μm. (d) 2% agarose electrophoresis of PCR products for the neomycin cassette performed on DNA extracted from spleens taken from mice transplanted with B6 (B6 Trx) or Alox15 (ATrx) cells versus Alox15 tail DNA positive control. (e) Table summarizing transfer experiments performed as described in panel a. Splenic distortion was assessed blindly. All error bars represent means ± SD.

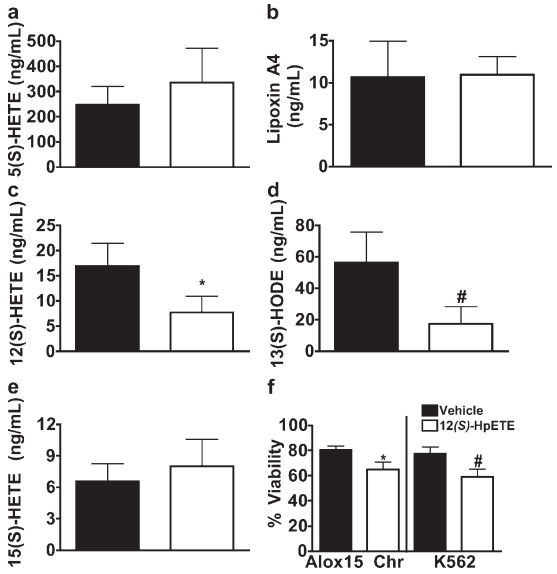

Figure 6. 12/15-LO–deficient MPD may be due in part to the loss of lipid mediators. Mass spectrometric or (in the case of lipoxin A_4) ELISA analysis of the release per mg of tissue of (a) 5*(S)*-HETE, (b) lipoxin A_4, (c) 12*(S)*-HETE, (d) 13*(S)*-HODE, and (e) 15*(S)*-HETE in PMA and ionomycin-stimulated unperfused spleens ($n = 4$). *, $P = 0.0058$; #, $P = 0.0006$. Shaded and open bars represent C57BL/6 and chronic Alox15 mice, respectively. (f) 24-h viability in Alox15 chronic(Chr) or K562 cells treated overnight with 60 μM 12(*S*)-HpETE, a direct 12/15-LO product. *, $P = 0.013$ ($n = 3$); #, $P = 0.003$ ($n = 3$). All error bars represent means ± SD.

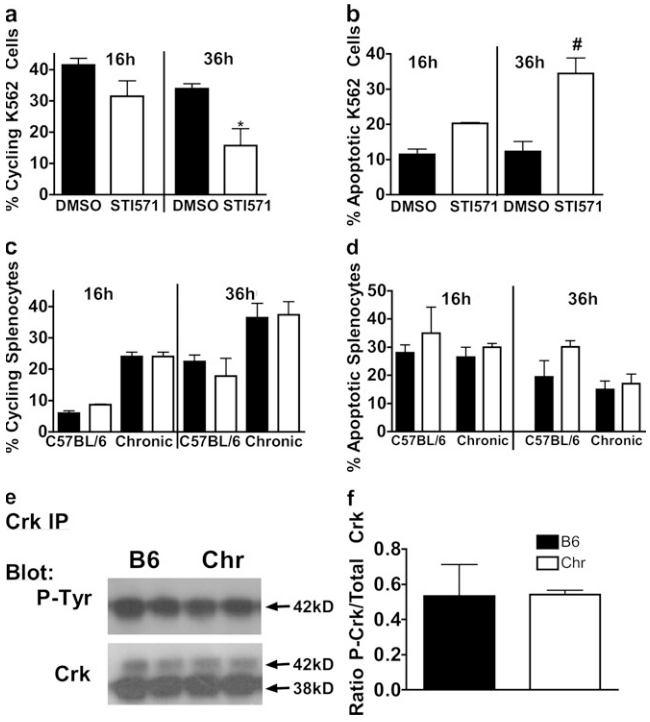

Figure 7. Alox15 MPD is Abl independent. Quantification of (a) cycling and (b) apoptotic K562 cells treated for the indicated times with 16 μM STI571 or DMSO vehicle control. *, $P = 0.036$ compared with DMSO control ($n = 3$); #, $P = 0.042$ compared with DMSO control ($n = 3$). Quantification of (c) cycling and (d) apoptotic cells in C57BL/6 wild-type or chronic Alox15 (Chr) splenocytes treated for the indicated times with 16 μM STI571 or DMSO vehicle control ($n = 3$). (e) Crk immunoprecipitation (IP) and immunoblot for phosphotyrosine (P-tyr) or Crk loading control of cytoplasmic lysates prepared from B6 and chronic Alox15 splenocytes ($n = 4$). (f) Quantification of the data shown in e. All error bars represent means ± SD.

substrate CrkL, to assess whether endogenous Abl activity was increased, as endogenous Abl may not be capable of phosphorylating CrkL to the degree that Bcr-Abl can (33). Nonetheless, we detected levels of phosphorylation of the major Abl substrate Crk that were comparable to the wild type (Fig. 7, c and d). Thus, at least in the ex vivo environment, the Alox15 MPD is independent of Abl activity.

Dysregulation of ICSBP and enhanced Bcl-2 expression in myeloid cells isolated from Alox15 mice

Given the importance of ICSBP in MPD (15), as well as our previous data demonstrating the ability of 12/15-LO to regulate ICSBP in other contexts (34), we hypothesized that 12/15-LO affects hematopoiesis by regulating ICSBP. Consistent with this hypothesis, we found that ICSBP nuclear levels were reduced in splenocytes from Alox15 mice and were barely detectable in splenocytes from mice that had progressed to blast crisis (Fig. 8 a). Real-time PCR for ICSBP revealed that its transcript levels in chronic stage Alox15 mice were comparable to the wild type, suggesting posttranslational regulation of ICSBP in this phase of the disease. On the other hand, expression of the ICSBP gene was nearly ablated in splenocytes isolated from mice in crisis (Fig. 8 b). This suggests that ICSBP is differentially regulated between the chronic and crisis stages of Alox15 MPD and that ICSBP expression inversely correlates with disease progression in Alox15 mice, as in the case of CML (16). As the decreased ICSBP expression in blast crisis mice was on an RNA level and, thus, caused by the gain of genetic mutations or transcriptional dysregulation that may complicate the interpretation of our experiments, we have focused our efforts in this study on elucidating the posttranslational mechanisms by which 12/15-LO regulates ICSBP in chronic stage Alox15 cells.

To investigate chronic stage Alox15 MPD, it was important to confirm that the decrease in nuclear levels of ICSBP in unfractionated chronic stage Alox15 splenocytes was a reflection of ICSBP dysregulation in chronic stage Alox15 myeloid cells. To do this, we examined the levels of ICSBP in enriched populations. Consistent with the RNA levels we observed in unfractionated spleens, chronic stage myeloid cells expressed similar ICSBP transcripts to wild-type controls (Fig. 8 c). However, we detected considerably lower nuclear levels of ICSBP protein in the Mac-1^+/GR-1^+ splenocyte populations isolated from Alox15 mice compared with those isolated from wild-type mice (Fig. 8 d). In contrast, the cytoplasmic levels of ICSBP in Alox15 myeloid cells were comparable to the wild type, indicating a nuclear accumulation defect (Fig. 8 d). The selectively decreased nuclear levels of

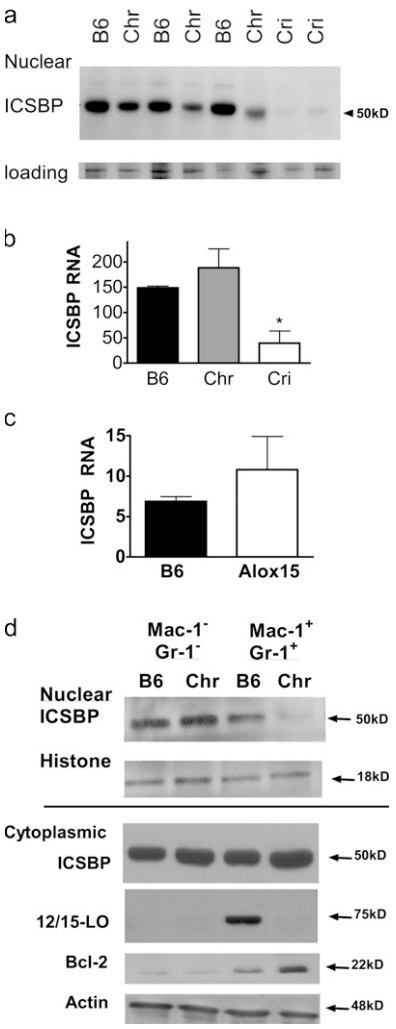

Figure 8. ICSBP defect and enhanced Bcl-2 expression in cells from Alox15 mice. (a) Immunoblot of nuclear extracts prepared from wild-type (B6), chronic Alox15 (Chr), and crisis Alox15 (Cri) splenocytes using antibodies specific for ICSBP and normalized to total protein, as confirmed by coomassie stain (loading). (b) Real-time PCR analysis of ICSBP mRNA expression levels in wild-type, chronic Alox15, and crisis Alox15 splenocytes. *, $P = 0.0115$ and 0.0284 compared with B6 and Chr, respectively. (c) Real-time PCR of sorted myeloid splenocytes isolated from C57BL/6 and chronic stage Alox15 mice. (d) Representative immunoblot of nuclear (above line) and cytoplasmic (below line) extracts prepared from sorted wild-type and Alox15 splenocytes for ICSBP, 12/15-LO, Bcl-2, and the loading controls histone 2b and total actin. The results are representative of three experiments. All error bars represent means ± SD.

ICSBP in the myeloid population, compared with the Mac-1^-/GR-1^- population, reinforce the conclusion that the aberrant cells in Alox15 mice are contained within the myeloid compartment, which is consistent with the selective expression of 12/15-LO in the myeloid lineage (Fig. 8 d).

To ascertain whether the regulation of ICSBP nuclear accumulation by 12/15-LO corresponds with changes in the expression of ICSBP target genes, we measured levels of Bcl-2, an oncoprotein known to be suppressed by ICSBP (19, 35), in myeloid cells. We observed a dramatic upregulation of Bcl-2 in the Alox15 myeloid population (Fig. 8 d) that correlated inversely with the nuclear accumulation of ICSBP.

PI3-K regulates Alox15 myeloproliferative cell survival and ICSBP phosphorylation and nuclear accumulation

Given the impact of tyrosine phosphorylation events on the ability of ICSBP to serve as a repressor of gene expression (36), we postulated that 12/15-LO regulates the nuclear accumulation and function of this transcription factor by influencing its phosphorylation status. Indeed, immunoprecipitation studies revealed an increase in tyrosine phosphorylation of ICSBP in Alox15 spleen (Fig. 9 a), indicating an important role for 12/15-LO in suppressing ICSBP phosphorylation.

Because the PI3-K pathway can promote Abl-independent CML, and in view of the capacity of 12/15- LO to regulate PI3-K in other settings (37), we explored the possibility that the dysregulation of ICSBP in Alox15 cells is PI3-K dependent. Indeed, we found increased levels of phosphorylation of the PI3-K pathway product Akt in bone marrow myeloid cells from Alox15 mice (Fig. 9 b). Conversely, treatment with the PI3-K inhibitor Ly294002 suppressed ICSBP phosphorylation and restored nuclear levels of ICSBP to that of the wild type (Fig. 9, c–f). This led to a correction in Bcl-2 transcript levels in Alox15 myeloid cells and induction of apoptosis in these cells within 24 h (Fig. 9, g and h). These data establish a mechanistic link between PI3-K and ICSBP and indicate that 12/15-LO regulates myeloid leukemogenesis by affecting the PI3-K signaling pathway.

DISCUSSION

This study establishes 12/15-LO as a critical and somewhat unexpected regulator in the suppression of MPD. We also place 12/15-LO in mechanistic context by demonstrating its impact on the phosphorylation and nuclear localization of ICSBP, as well as that the ICSBP dysregulation in and survival of aberrant Alox15 cells is PI3-K dependent.

We found that Alox15 mice older than 10 wk develop MPD with 100% penetrance. In considering a novel mouse model for leukemic disease, it is important to evaluate the preleukemic state, pathology in knockouts as well as controls, and to assess the transferability of the leukemic syndrome (29), all of which we have done. However, one should, if possible, also investigate whether the disease is clonal in nature using antigen receptor rearrangement or retroviral insertion sites. Unfortunately, given the strictly myeloid nature of the syndrome in our mice and the fact that these animals are free of retroviral insertions, none of the conventional methods were available to us to establish clonality (29). Therefore, though the persistence of transplanted Alox15 cells 10 wk after transfer to wild-type recipients strongly suggests the clonal derivation of these cells, we have opted to make the more conservative conclusion that Alox15 mice develop a MPD that may become leukemic. Further studies, perhaps using a nontransforming retrovirus, will be required to completely elucidate this issue.

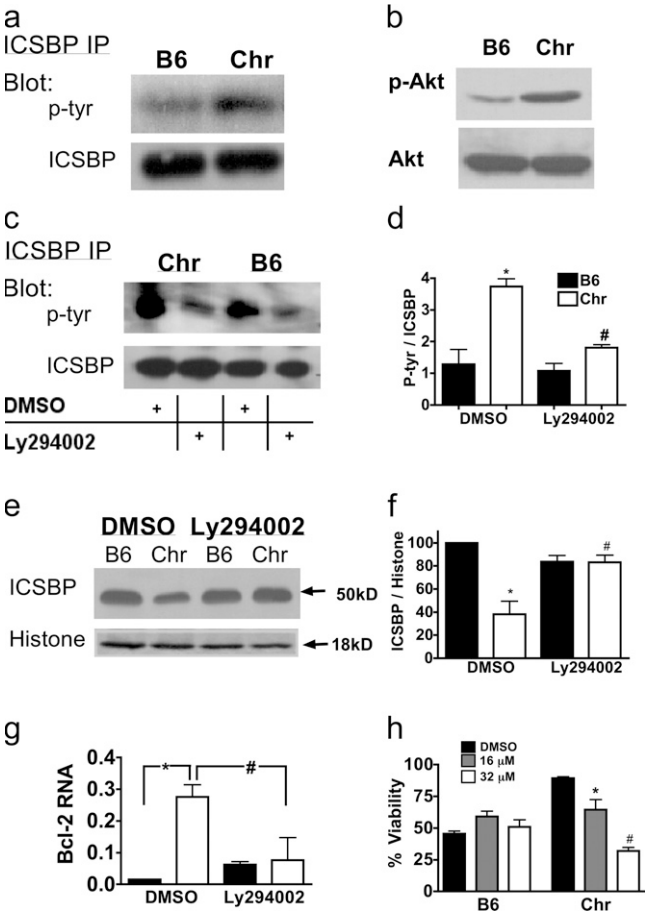

Figure 9. PI3-K regulates Alox15 myeloproliferative cell survival and ICSBP phosphorylation and nuclear accumulation. (a) Immunoblot of ICSBP immunoprecipitated from wild-type (B6) and chronic Alox15 (Chr) splenocyte total lysates. (b) Constitutive levels of phosphorylated Akt in bone marrow myeloid cells cultured for 5 d in GM-CSF. (c) Splenocytes were cultured for 6 h in 16 μM Ly296002 or DMSO vehicle control, and samples were prepared and analyzed as in panel a. (d) Quantification of the data shown in c ($n = 3$). *, $P = 0.0012$ compared with B6 DMSO; #, $P = 0.0081$ compared with Chr DMSO. (e) Nuclear extracts of cells treated as in c. (f) Quantification of the data shown in e ($n = 3$). *, $P = 0.0052$ compared with B6 DMSO; #, $P = 0.0155$ compared with Chr DMSO. (g) Real-time PCR of Bcl-2 transcripts in sorted myeloid splenocytes from C57BL/6 and Alox15 cells. *, $P = 0.001$; #, $P = 0.02$. (h) Quantification of splenocyte viability by trypan blue exclusion after 24-h culture of B6 and Chr splenocytes with Ly294002 or DMSO control ($n = 3$). *, $P = 0.0326$ compared with B6 DMSO; #, $P = 0.006$ compared with B6 DMSO. All error bars represent means ± SD.

Given the indolent nature of the MPD that occurs in Alox15 mice, these animals provide a relatively unique opportunity to study the mechanisms underlying the chronic stage of MPD and its transition to blast crisis. In fact, as with humans with CML, we have found in this study that ICSBP is regulated differently in chronic and crisis stage cells, which appears to affect downstream targets of this transcription factor. In the future, it will be important to distinguish whether the switch to crisis is a result of transcriptional regulation of ICSBP by 12/15-LO or is caused by mutations in this gene. Indeed, it is possible that the occurrence of genetic aberrancies in ICSBP are a prerequisite of blastic transformation given the near uniform reduction in ICSBP transcripts in patients with crisis stage CML (16). Thus, further studies to define mechanisms of blastic transformation in indolent models of CML such as Alox15 mice are critical to developing new therapies. Moreover, as we have shown that 12/15-LO is expressed selectively in the myeloid lineage among hematopoietic cells, this pathway may present a selective target for treating MPD.

Curiously, though Alox15 mice were generated nearly a decade ago, the MPD we describe in this manuscript was not previously reported. There are several possible explanations for this. One possibility is that the syndrome in Alox15 may have become more pronounced on the pure C57BL/6 genetic background described in this study, as opposed to the F = 7 animals previously studied. Additionally, the majority of Alox15 mice manifests a degree of splenomegaly that might not be obvious to investigators handling the mice for other purposes and, therefore, who are not focused on the integrity of lymphoid organs. This is less likely in the case of the more dramatic splenomegaly observed in mice in blast crisis, but the incidence of these mice is relatively low (~15%). Importantly, scientists at the Jackson Laboratory, the vendor of Alox15 mice (see Materials and methods), have recently examined Alox15 mice versus wild-type controls and have observed a similar phenotype of splenomegaly and flow cytometric abnormalities, confirming our findings in an independent facility (Nicholson, A., personal communication). The history of Alox15 mice mirrors the plight of human CML patients who, because of their initially mild symptoms, are often considered healthy for some time before being diagnosed.

We demonstrated that 12/15-LO–mediated suppression of leukemic cell growth is dependent on its enzymatic activity, and our ex vivo data suggest that 12/15-LO is responsible for producing several lipid mediators in vivo, including 12*(S)*-HETE. Interestingly, others have shown decreased levels of 12*(S)*-HETE in the bone marrow of humans with CML (21). This effect may be caused in part by reduced levels of platelet 12-lipoxygenase RNA levels in CML patients (22). The common products between leukocyte and platelet 12-lipoxygenases likely explain the fact that these enzymes are often jointly implicated in disease pathology, as exemplified in the case of osteoporosis (38, 39). Another reason for the overlapping functions between these two enzymes may be transcellular oxidation products formed between platelets and leukocytes, such as lipoxins and their intermediates (40–42). Alternatively, other consequences of lipoxygenase activity, such as direct membrane oxidation and reactive oxygen species, may be involved (20).

Consistent with the mechanistic links between them, the ICSBP and 12/15-LO–deficient mouse models for human MPD share several characteristics. Indeed, the decreased survival in ICSBP heterozygotes (9%) (15) is similar to what we observed in 12/15-LO–null mice, which would be expected

in the context of the reduced (but not completely ablated) nuclear levels of ICSBP observed in 12/15-LO–deficient animals. Both models also display an initial MPD that transitions to a transplantable leukemia in a subset of animals over time. Additionally, it is important to note that both ICSBP and 12/15-LO are involved in inflammation (43–46), which may mediate in part their effects on leukemic disease, as many contemporary studies indicate that there may be a stronger connection between inflammation and carcinogenesis than previously recognized (47). Finally, mouse ICSBP and 12/15-LO share a high degree of homology with their human counterparts (48, 49), each are down-regulated in cells from CML patients (16, 21), and both can suppress human CML growth; therefore, both of these molecules are mechanistically relevant to human pathology. The lack of requirement for Abl activation in the 12/15-LO and ICSBP-deficient models is of particular interest considering the resistance to Abl inhibitors in a substantial proportion of myeloid leukemia patients and the role of the PI3-K pathway in many of these cases (9).

PI3-K is activated by cellular stress and various cytokine pathways, promoting cell survival, metabolism, and growth (50). Mice deficient in PTEN, a suppressor of PI3-K–mediated Akt activation, succumb to myeloid leukemias (51). Moreover, PI3-K inhibitors have been shown to kill imatinib-resistant leukemic cells, underscoring the importance of the PI3-K pathway in CML. However, because activation of PI3-K can be both Abl-dependent and -independent (9, 52), the PI3-K–dependent nature of the Alox15 syndrome does not readily elucidate whether 12/15-LO may be acting downstream of or in parallel to the Abl signaling cascade.

The role of 12/15-LO in regulating PI3-K signaling, especially in myeloid cells, was previously unknown. However, others have shown that the 12/15-LO products 13(*S*)-HODE and 15(*S*)-HETE up- and down-regulate, respectively, Akt phosphorylation in prostate cells (37), whereas 12/15-LO products uniformly up-regulate Akt phosphorylation in vascular smooth muscle cells (53). Thus, a cell-type selective effect of 12/15-LO on PI3-K signaling is apparent and will be of great interest to study in myeloid cells.

We have demonstrated decreased nuclear accumulation of ICSBP in Alox15 myeloid cells, which may be the result of PI3-K–mediated aberrant phosphorylation of ICSBP. In agreement with our study, it has been reported that tyrosine phosphorylation of ICSBP can decrease its direct binding to DNA, thereby limiting its ability to repress gene transcription (36). However, this phosphorylation also increases its binding to other transcription factors (36), enabling ICSBP to induce gene expression. Indeed, others have shown that phosphorylation of ICSBP on tyrosines 92 and 95 promotes its positive regulation of neurofibromin 1 expression without affecting ICSBP suppressor function, thereby promoting myeloid cell differentiation in vitro (54, 55). On the other hand, our data suggest that increased tyrosine phosphorylation of ICSBP can also promote MPD, likely through acting on distinct tyrosines. Thus, it will be important in future studies to characterize which tyrosine residues are phosphorylated as a result of 12/15-LO–mediated PI3-K pathway activity. In either case, the increased phosphorylation of ICSBP in our model may either subject it to a more rapid nuclear turnover secondary to decreased DNA binding or directly suppress its nuclear translocation. Our working model of the 12/15-LO–dependent regulation of ICSBP is presented in Fig. 10.

In addition to mouse MPD, several observations signify a potentially important role for 12/15-LO in human CML. 12/15-LO is expressed in human hematopoietic tissues and myeloid cells, its products are both diminished in and can suppress human myeloid leukemia (21), and the Alox15 locus maps to a region of chromosome 17p13 implicated in human myeloid leukemogenesis (23). Though a few other candidate genes are being considered on chromosome 17, our study represents the first direct evidence of the involvement of a particular locus in this susceptibility region in myeloid leukemia. Thus, it is of great interest to determine whether, as our data and that of others suggest, the Alox15 gene is mutated in human myeloid leukemias. We are currently investigating this possibility.

Further dissecting the mechanism by which 12/15-LO suppresses MPD will uncover novel regulatory pathways in hematopoiesis and may pave the way for the development of additional targeted therapies for the treatment of myeloid leukemias and other cancers.

MATERIALS AND METHODS

Mice, cells, and reagents. C57BL/6 and Alox15 mice on a C57BL/6 background (backcrossed 11 generations) were purchased from The Jackson Laboratory and housed and bred in the Wistar Institute Animal Facility. Severe combined immunodeficiency mice were purchased from the Wistar Institute Animal Facility. All animals were treated in accordance with a Wistar Institute protocol approved by the institutional animal care and use committee. K562 cells were purchased from the American Type Culture Collection. Ly294002 and PD146176 were purchased from Calbiochem and Sigma-Aldrich, respectively. STI571 was supplied by Novartis. K562 cells were nucleofected (Amaxa) according to the manufacturer's optimized protocol.

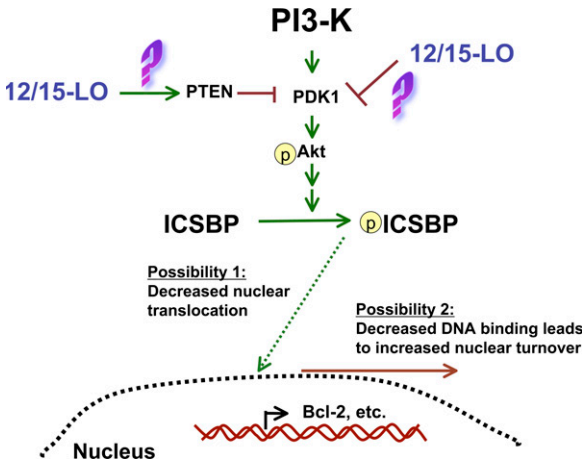

Figure 10. Potential mechanisms by which 12/15-LO may regulate ICSBP. Absence of 12/15-LO leads to increased PI3-K pathway activation, possibly via loss of inhibition of activators such as PDK1 or gain of activity of PTEN. PI3-K–dependent phosphorylation of ICSBP may reduce nuclear levels by diminished nuclear translocation, increased nuclear turnover, or both.

Lipid quantification. Unperfused fresh spleens were cut into sections in duplicate and stimulated for 20 min with 1 μM ionomycin and 200 nM PMA in serum-free media. Some of the supernatant was used for lipoxin A_4 analysis by ELISA (Oxford Biomedical Research, Inc.). The rest of the supernatant was extracted for analysis by stable isotope dilution normal phase chiral liquid chromatography (LC) coupled with electron capture atmospheric pressure chemical ionization (APCI)/mass spectrometry (MS) as described previously (49). In brief, samples were spiked with deuterium-labeled internal standards, adjusted to pH 3 with 2.5 N hydrochloric acid, and extracted with 2 × 4 ml diethyl ether. The organic layer was evaporated to dryness under nitrogen, derivatized with 2,3,4,5,6-pentafluorobenzyl bromide in the presence of diisopropylethylamine, and evaporated to dryness under a stream of nitrogen. Derivatized samples were reconstituted in 100 μl of hexane/ethanol (97:3, vol/vol) and 20 μl was analyzed by LC/electron capture APCI/MS system for analysis. Quantitation was performed by comparison of peak area ratios of the analytes to their relevant stable isotope internal standard and interpolation of area ratios from a standard curve (49).

Transfer experiments. 8–10-wk-old wild-type mice were injected via the tail vein with 0.5×10^6 (Alox15 crisis) or 10^7 (Alox15 chronic and C57BL/6) splenocytes or 2×10^6 bone marrow cells, monitored every other day, and killed at 6 or 10 wk after transfer. Tumor transfer was assessed by blinded morphological characterization of the spleens by hematoxylin and eosin (H&E). The presence of Alox15 donor cells in the transplanted mice was confirmed by PCR of the spleen DNA with primers specific for the neomycin cassette introduced by the Alox15 targeting construct (see Primer sequences).

Histology. Blood samples were collected from the inferior vena cava, anticoagulated with EDTA, and kept on ice before slide preparation. Bone marrow cells were collected by flushing the femurs of wild-type and Alox15 mice. Cytospin slides were stained using Kwik-Diff reagents for Wright stains (Thermo Electron). Tissue samples were frozen in Tissue-Tek OCT and stored at −80°C. Morphology was analyzed in 8-μm sections stained with Gill's H&E. Tdt-mediated dUTP-biotin nick-end labeling staining for apoptotic cells was performed on three sections of spleen per mouse using a staining kit (Roche Applied Science) according to the manufacturer's instructions. The number of positive cells was quantified using Image-Pro software (Media Cybernetics).

Flow cytometry. Single cell suspensions of splenocytes, bone marrow cells, and Histopaque 1083–purified (Sigma-Aldrich) peripheral mononuclear cells were prepared and depleted of red blood cells by lysis in ammonium chloride buffer, and cells were stained using 2 μg/ml directly labeled specific antibody or isotype-matched antibodies as controls. Compensation was performed using anti-CD4 or Mac-1 (FITC) and anti-CD8 or Mac-1 (PE) staining. All flow cytometric antibodies were purchased from BD Biosciences. Cells were washed and analyzed using a BD FACSCalibur machine (BD Biosciences). For sorting, cells were stained as described earlier in this paragraph and sorted for the populations indicated in the figures at the Wistar Institute Flow Cytometry Core facility.

Propidium iodide staining. Single cell suspensions were fixed in ice-cold 70% ethanol at 4C° for 1 h, washed with PBS, and resuspended in 50 μg/ml propidium iodide containing 1.5 mM sodium citrate and 5 μg/ml RNase A in PBS. Samples were analyzed by flow cytometry.

Lysates, immunoprecipitation, and Western blots. RBC-depleted splenocytes were prepared as in Flow cytometry, and nuclear lysates were prepared using the NucBuster kit (EMD Biosciences) according to the manufacturer's instructions. For cytoplasmic lysates, extracts were prepared from isolated cells using 1% NP-40 lysis buffer with phosphatase and protease inhibitors, whereas total extracts were prepared using M-PER (Bio-Rad Laboratories) according to manufacturer's instructions. For immunoprecipitation, extracts were normalized to total protein concentration using a Bradford assay (Bio-Rad Laboratories), according to manufacturer's instructions, and immunoprecipitated overnight with 1 μg of antibody, captured with protein G beads, and washed five times with 0.1% SDS buffer before electrophoresis. For Western analysis of unprecipitated extracts, samples were normalized to total protein using Bradford assay according to manufacturer's instructions, resolved by 10% SDS page gel electrophoresis, transferred to polyvinylidene difluoride membranes, and immunoblotted with specific antibodies, as described in Results. All immunoblotting antibodies were obtained from Santa Cruz Biotechnology, Inc., except the anti-Crk antibody, which was purchased from BD Biosciences, and anti-phosphoAkt (Ser473), which was purchased from Cell Signaling.

Reverse transcription reaction/quantitative real-time PCR. Total RNA was extracted from splenocytes using TRIzol (Invitrogen) according to manufacturer's instructions. RNA was treated with Turbo DNase (Ambion) according to the manufacturer's instructions to remove any contaminating genomic DNA, and the absence of appreciable genomic DNA was confirmed by real-time PCR of the treated RNA. RNA was normalized by OD, and reverse transcription reaction was performed using a cDNA synthesis kit (Applied Biosystems) according to the manufacturer's instructions. Quantitative real-time PCR analysis was performed using Sybr green Master Mix (Applied Biosystems) and analyzed using the ABI 7000 machine (Applied Biosystems). Gene-specific primers (see the next paragraph) were designed using Primer Express (Applied Biosystems), and gene expression levels were normalized using β-actin as an internal control.

Primer sequences. The following primer sequences were used: β-actin, (forward) 5′−TCAGCAAGCAGGAGTACGATG-3′ and (reverse) 5′−AACAGTCCGCCTAGAAGCACTT-3′; ICSBP (forward) 5′-TGGGCAGTTTTTAAAGGGAAGTT-3′ and (reverse) 5′-ACAGCGTAACCTCGTCTTCCA-3′; 12/15-LO (forward) 5′-ACCCCACCGCCGATTTT and (reverse) 5′-AGCTTCGGACCCAGCATTT; and neomycin cassette (forward) 5′-TTGGGTGGAGAGGCTATTCG-3′ and (reverse) 5′-AACACGGCGGCATCAGA-3′.

Statistical analysis. One-way analysis of variance (for comparing more than two groups) and *t*-tests (for comparing two groups) were calculated using Prism software (GraphPad) according to the program's designation of the most statistically valid test for each experiment. The α level was set at 0.05 for all tests; p-values below this were considered statistically significant. All error bars represent means ± SD.

Online supplemental material. Fig. S1 shows comparable hematopoietic compartments to wild-type controls in young Alox15 mice. Fig. S2 depicts increased megakaryocytes and decreased red blood cell numbers in Alox15 mice. Fig. S3 shows myeloid infiltrates in the skin of moribund Alox15 mice. Online supplemental material is available at http://www.jem.org/cgi/content/full/jem.20061444/DC1.

We thank Drs. Warren Pear, John Choi, Nina Luning Prak, and Jason Hall for evaluation of this manuscript. We also acknowledge the generous technical support of the following members of the Wistar Institute: Irene Crichton for lab management; Adrienne Whitmore (deceased) for assistance with graphics; Sonali Majumdar for technical assistance; the Flow Cytometry, Microscopy, and Histology Core Facilities; and Information Systems. Alicia M. Zukas contributed to the histological analysis and participated in scientific discussion. Tanya Rubinstein contributed to animal dissections and scientific discussion. Michele Jacob developed and optimized the Crk phosphorylation assay and contributed to scientific discussion. Peijuan Zhu and Ian Blair assisted with the execution, analysis, and interpretation of the liquid chromatography/mass spectrometry. Liang Zhao assisted with the transfer experiments and histology.

These studies were funded by Public Health Service grants R01AI45813 and T32CA01940 (to E. Puré) and National Institutes of Health grant R01CA 91016 (to I.A. Blair), as well as a grant from the Pennsylvania Department of Health.

The authors have no conflicting financial interests.

Submitted: 7 July 2006
Accepted: 27 September 2006

REFERENCES

1. Kantarjian, H., J.V. Melo, S. Tura, S. Giralt, and M. Talpaz. 2000. Chronic myelogenous leukemia: disease biology and current and future therapeutic strategies. *Hematology (Am. Soc. Hematol. Educ. Program)*. 2000:90–109.
2. Wertheim, J.A., J.P. Miller, L. Xu, Y. He, and W.S. Pear. 2002. The biology of chronic myelogenous leukemia: mouse models and cell adhesion. *Oncogene*. 21:8612–8628.
3. Cohen, M.H., J.R. Johnson, and R. Pazdur. 2005. U.S. Food and Drug Administration Drug Approval Summary: conversion of imatinib mesylate (STI571; Gleevec) tablets from accelerated approval to full approval. *Clin. Cancer Res*. 11:12–19.
4. Hochhaus, A., and T. Hughes. 2004. Clinical resistance to imatinib: mechanisms and implications. *Hematol. Oncol. Clin. North Am*. 18:641–656 (ix.).
5. Michor, F., T.P. Hughes, Y. Iwasa, S. Branford, N.P. Shah, C.L. Sawyers, and M.A. Nowak. 2005. Dynamics of chronic myeloid leukaemia. *Nature*. 435:1267–1270.
6. Mughal, T.I., and J.M. Goldman. 2006. Chronic myeloid leukemia: why does it evolve from chronic phase to blast transformation? *Front. Biosci*. 11:198–208.
7. Bacher, U., T. Haferlach, W. Hiddemann, S. Schnittger, W. Kern, and C. Schoch. 2005. Additional clonal abnormalities in Philadelphia-positive ALL and CML demonstrate a different cytogenetic pattern at diagnosis and follow different pathways at progression. *Cancer Genet. Cytogenet*. 157:53–61.
8. Harris, N.L., E.S. Jaffe, J. Diebold, G. Flandrin, H.K. Muller-Hermelink, J. Vardiman, T.A. Lister, and C.D. Bloomfield. 1999. World Health Organization classification of neoplastic diseases of the hematopoietic and lymphoid tissues: report of the Clinical Advisory Committee meeting-Airlie House, Virginia, November 1997. *J. Clin. Oncol*. 17:3835–3849.
9. Burchert, A., Y. Wang, D. Cai, N. von Bubnoff, P. Paschka, S. Muller-Brusselbach, O.G. Ottmann, J. Duyster, A. Hochhaus, and A. Neubauer. 2005. Compensatory PI3-kinase/Akt/mTor activation regulates imatinib resistance development. *Leukemia*. 19:1774–1782.
10. Parmar, S., E. Katsoulidis, A. Verma, Y. Li, A. Sassano, L. Lal, B. Majchrzak, F. Ravandi, M.S. Tallman, E.N. Fish, and L.C. Platanias. 2004. Role of the p38 mitogen-activated protein kinase pathway in the generation of the effects of imatinib mesylate (STI571) in BCR-ABL-expressing cells. *J. Biol. Chem*. 279:25345–25352.
11. Passegue, E., E.F. Wagner, and I.L. Weissman. 2004. JunB deficiency leads to a myeloproliferative disorder arising from hematopoietic stem cells. *Cell*. 119:431–443.
12. Pear, W.S., J.P. Miller, L. Xu, J.C. Pui, B. Soffer, R.C. Quackenbush, A.M. Pendergast, R. Bronson, J.C. Aster, M.L. Scott, and D. Baltimore. 1998. Efficient and rapid induction of a chronic myelogenous leukemia-like myeloproliferative disease in mice receiving P210 bcr/abl-transduced bone marrow. *Blood*. 92:3780–3792.
13. Koschmieder, S., B. Gottgens, P. Zhang, J. Iwasaki-Arai, K. Akashi, J.L. Kutok, T. Dayaram, K. Geary, A.R. Green, D.G. Tenen, and C.S. Huettner. 2005. Inducible chronic phase of myeloid leukemia with expansion of hematopoietic stem cells in a transgenic model of BCR-ABL leukemogenesis. *Blood*. 105:324–334.
14. Metcalf, D. 2006. Loss of PU.1: one of the many roads to myeloid leukemia. *Cell Cycle*. 5:673–674.
15. Holtschke, T., J. Lohler, Y. Kanno, T. Fehr, N. Giese, F. Rosenbauer, J. Lou, K.P. Knobeloch, L. Gabriele, J.F. Waring, et al. 1996. Immunodeficiency and chronic myelogenous leukemia-like syndrome in mice with a targeted mutation of the ICSBP gene. *Cell*. 87:307–317.
16. Schmidt, M., S. Nagel, J. Proba, C. Thiede, M. Ritter, J.F. Waring, F. Rosenbauer, D. Huhn, B. Wittig, I. Horak, and A. Neubauer. 1998. Lack of interferon consensus sequence binding protein (ICSBP) transcripts in human myeloid leukemias. *Blood*. 91:22–29.
17. Hao, S.X., and R. Ren. 2000. Expression of interferon consensus sequence binding protein (ICSBP) is downregulated in Bcr-Abl-induced murine chronic myelogenous leukemia-like disease, and forced coexpression of ICSBP inhibits Bcr-Abl-induced myeloproliferative disorder. *Mol. Cell. Biol*. 20:1149–1161.
18. Tamura, T., H.J. Kong, C. Tunyaplin, H. Tsujimura, K. Calame, and K. Ozato. 2003. ICSBP/IRF-8 inhibits mitogenic activity of p210 Bcr/Abl in differentiating myeloid progenitor cells. *Blood*. 102:4547–4554.
19. Burchert, A., D. Cai, L.C. Hofbauer, M.K. Samuelsson, E.P. Slater, J. Duyster, M. Ritter, A. Hochhaus, R. Muller, M. Eilers, et al. 2004. Interferon consensus sequence binding protein (ICSBP; IRF-8) antagonizes BCR/ABL and down-regulates bcl-2. *Blood*. 103:3480–3489.
20. Conrad, D.J. 1999. The arachidonate 12/15 lipoxygenases. A review of tissue expression and biologic function. *Clin. Rev. Allergy Immunol*. 17:71–89.
21. Stenke, L., L. Lauren, P. Reizenstein, and J.A. Lindgren. 1987. Leukotriene production by fresh human bone marrow cells: evidence of altered lipoxygenase activity in chronic myelocytic leukemia. *Exp. Hematol*. 15:203–207.
22. Stenke, L., C. Edenius, J. Samuelsson, and J.A. Lindgren. 1991. Deficient lipoxin synthesis: a novel platelet dysfunction in myeloproliferative disorders with special reference to blastic crisis of chronic myelogenous leukemia. *Blood*. 78:2989–2995.
23. Sankar, M., K. Tanaka, T.S. Kumaravel, M. Arif, T. Shintani, S. Yagi, T. Kyo, H. Dohy, and N. Kamada. 1998. Identification of a commonly deleted region at 17p13.3 in leukemia and lymphoma associated with 17p abnormality. *Leukemia*. 12:510–516.
24. Biermann, H., B. Pietz, R. Dreier, K.W. Schmid, C. Sorg, and C. Sunderkotter. 1999. Murine leukocytes with ring-shaped nuclei include granulocytes, monocytes, and their precursors. *J. Leukoc. Biol*. 65:217–231.
25. Vainchenker, W., J. Guichard, J.F. Deschamps, J. Bouguet, M. Titeux, J. Chapman, A.J. McMichael, and J. Breton-Gorius. 1982. Megakaryocyte cultures in the chronic phase and in the blast crisis of chronic myeloid leukaemia: studies on the differentiation of the megakaryocyte progenitors and on the maturation of megakaryocytes in vitro. *Br. J. Haematol*. 51:131–146.
26. Busche, G., H. Majewski, J. Schlue, S. Delventhal, S. Baer-Henney, K.F. Vykoupil, and A. Georgii. 1997. Frequency of pseudo-Gaucher cells in diagnostic bone marrow biopsies from patients with Ph-positive chronic myeloid leukaemia. *Virchows Arch*. 430:139–148.
27. Kaddu, S., P. Zenahlik, C. Beham-Schmid, H. Kerl, and L. Cerroni. 1999. Specific cutaneous infiltrates in patients with myelogenous leukemia: a clinicopathologic study of 26 patients with assessment of diagnostic criteria. *J. Am. Acad. Dermatol*. 40:966–978.
28. Klein, E., H. Ben-Bassat, H. Neumann, P. Ralph, J. Zeuthen, A. Polliack, and F. Vanky. 1976. Properties of the K562 cell line, derived from a patient with chronic myeloid leukemia. *Int. J. Cancer*. 18:421–431.
29. Metcalf, D. 2005. Blood Lines: An Introduction to Characterizing Blood Diseases of the Post-Genomic Mouse. AlphaMed Press, Durham, NC. 251 pp.
30. Li, X., N. Qiao, D. Reynaud, M. Abdelhaleem, and C.R. Pace-Asciak. 2005. PBT-3, a hepoxilin stable analog, causes long term inhibition of growth of K562 solid tumours in vivo. *Biochem. Biophys. Res. Commun*. 338:158–160.
31. Kelliher, M.A., J. McLaughlin, O.N. Witte, and N. Rosenberg. 1990. Induction of a chronic myelogenous leukemia-like syndrome in mice with v-abl and BCR/ABL. *Proc. Natl. Acad. Sci. USA*. 87:6649–6653.
32. Feller, S.M., B. Knudsen, and H. Hanafusa. 1994. c-Abl kinase regulates the protein binding activity of c-Crk. *EMBO J*. 13:2341–2351.
33. Nichols, G.L., M.A. Raines, J.C. Vera, L. Lacomis, P. Tempst, and D.W. Golde. 1994. Identification of CRKL as the constitutively phosphorylated 39-kD tyrosine phosphoprotein in chronic myelogenous leukemia cells. *Blood*. 84:2912–2918.
34. Middleton, M.K., T. Rubinstein, and E. Puré. 2006. Cellular and molecular mechanisms of the selective regulation of IL-12 production by 12/15-lipoxygenase. *J. Immunol*. 176:265–274.
35. Gabriele, L., J. Phung, J. Fukumoto, D. Segal, I.M. Wang, P. Giannakakou, N.A. Giese, K. Ozato, and H.C. Morse III. 1999. Regulation of apoptosis in myeloid cells by interferon consensus sequence binding protein. *J. Exp. Med*. 190:411–421.
36. Sharf, R., D. Meraro, A. Azriel, A.M. Thornton, K. Ozato, E.F. Petricoin, A.C. Larner, F. Schaper, H. Hauser, and B.Z. Levi. 1997.

Phosphorylation events modulate the ability of interferon consensus sequence binding protein to interact with interferon regulatory factors and to bind DNA. *J. Biol. Chem.* 272:9785–9792.
37. Hsi, L.C., L.C. Wilson, and T.E. Eling. 2002. Opposing effects of 15-lipoxygenase-1 and -2 metabolites on MAPK signaling in prostate. Alteration in peroxisome proliferator-activated receptor gamma. *J. Biol. Chem.* 277:40549–40556.
38. Ichikawa, S., D.L. Koller, M.L. Johnson, D. Lai, X. Xuei, H.J. Edenberg, R.F. Klein, E.S. Orwoll, S.L. Hui, T.M. Foroud, et al. 2006. Human ALOX12, but not ALOX15, is associated with BMD in white men and women. *J. Bone Miner. Res.* 21:556–564.
39. Klein, R.F., J. Allard, Z. Avnur, T. Nikolcheva, D. Rotstein, A.S. Carlos, M. Shea, R.V. Waters, J.K. Belknap, G. Peltz, and E.S. Orwoll. 2004. Regulation of bone mass in mice by the lipoxygenase gene Alox15. *Science.* 303:229–232.
40. Marcus, A.J. 1986. Transcellular metabolism of eicosanoids. *Prog. Hemost. Thromb.* 8:127–142.
41. Stenke, L., J. Samuelsson, J. Palmblad, L. Dabrowski, P. Reizenstein, and J.A. Lindgren. 1990. Elevated white blood cell synthesis of leukotriene C4 in chronic myelogenous leukaemia but not in polycythaemia vera. *Br. J. Haematol.* 74:257–263.
42. Schumacher, H.R., and J.R. Kos. 1982. Deficiency of platelet lipoxygenase activity in myeloproliferative disorders. *N. Engl. J. Med.* 307:378–379.
43. Middleton, M.K., T. Rubinstein, and E. Pure. 2006. Cellular and molecular mechanisms of the selective regulation of IL-12 production by 12/15-lipoxygenase. *J. Immunol.* 176:265–274.
44. Reilly, K.B., S. Srinivasan, M.E. Hatley, M.K. Patricia, J. Lannigan, D.T. Bolick, G. Vandenhoff, H. Pei, R. Natarajan, J.L. Nadler, and C.C. Hedrick. 2004. 12/15-Lipoxygenase activity mediates inflammatory monocyte/endothelial interactions and atherosclerosis in vivo. *J. Biol. Chem.* 279:9440–9450.
45. Huo, Y., L. Zhao, M.C. Hyman, P. Shashkin, B.L. Harry, T. Burcin, S.B. Forlow, M.A. Stark, D.F. Smith, S. Clarke, et al. 2004. Critical role of macrophage 12/15-lipoxygenase for atherosclerosis in apolipoprotein E-deficient mice. *Circulation.* 110:2024–2031.
46. Paintlia, A.S., M.K. Paintlia, I. Singh, and A.K. Singh. 2006. IL-4-induced peroxisome proliferator-activated receptor gamma activation inhibits NF-kappaB trans activation in central nervous system (CNS) glial cells and protects oligodendrocyte progenitors under neuroinflammatory disease conditions: implication for CNS-demyelinating diseases. *J. Immunol.* 176:4385–4398.
47. Karin, M., T. Lawrence, and V. Nizet. 2006. Innate immunity gone awry: linking microbial infections to chronic inflammation and cancer. *Cell.* 124:823–835.
48. Chen, X.S., U. Kurre, N.A. Jenkins, N.G. Copeland, and C.D. Funk. 1994. cDNA cloning, expression, mutagenesis of C-terminal isoleucine, genomic structure, and chromosomal localizations of murine 12-lipoxygenases. *J. Biol. Chem.* 269:13979–13987.
49. Weisz, A., P. Marx, R. Sharf, E. Appella, P.H. Driggers, K. Ozato, and B.Z. Levi. 1992. Human interferon consensus sequence binding protein is a negative regulator of enhancer elements common to interferon-inducible genes. *J. Biol. Chem.* 267:25589–25596.
50. Plas, D.R., and C.B. Thompson. 2005. Akt-dependent transformation: there is more to growth than just surviving. *Oncogene.* 24:7435–7442.
51. Zhang, J., J.C. Grindley, T. Yin, S. Jayasinghe, X.C. He, J.T. Ross, J.S. Haug, D. Rupp, K.S. Porter-Westpfahl, L.M. Wiedemann, et al. 2006. PTEN maintains haematopoietic stem cells and acts in lineage choice and leukaemia prevention. *Nature.* 441:518–522.
52. Kharas, M.G., and D.A. Fruman. 2005. ABL oncogenes and phosphoinositide 3-kinase: mechanism of activation and downstream effectors. *Cancer Res.* 65:2047–2053.
53. Li, F., and K.U. Malik. 2005. Angiotensin II-induced Akt activation is mediated by metabolites of arachidonic acid generated by CaMKII-stimulated $Ca2^{+}$-dependent phospholipase A2. *Am. J. Physiol. Heart Circ. Physiol.* 288:H2306–H2316.
54. Huang, W., G. Saberwal, E. Horvath, C. Zhu, S. Lindsey, and E.A. Eklund. 2006. Leukemia-associated, constitutively active mutants of SHP2 protein tyrosine phosphatase inhibit NF1 transcriptional activation by the interferon consensus sequence binding protein. *Mol. Cell. Biol.* 26:6311–6332.
55. Zhu, C., G. Saberwal, Y. Lu, L.C. Platanias, and E.A. Eklund. 2004. The interferon consensus sequence-binding protein activates transcription of the gene encoding neurofibromin 1. *J. Biol. Chem.* 279:50874–50885.
56. Pearson, E.C. 1989. Auer rods and myeloperoxidase: an approach for investigating changes at the molecular level in acute myeloid leukaemia (AML). *Med. Hypotheses.* 30:175–177.